# NUCLEAR   SAFETY AND RELIABILITY

**WEEK 9**

TABLE OF CONTENTS - WEEK 9

Space - Time Power Transient

The power transient produced by coolant voiding following a LOCA must be modeled in three dimensions in CANDU reactors, because of the local effects of reactivity changes on the neutron flux.   The time-dependent diffusion equation is:

$$\left[ -M + F^p \right] \phi(\bar{r},t) + \sum_1 \lambda_i C_i(\bar{r},t) = \frac{1}{v} \frac{\partial \phi(\bar{r},t)}{\partial t}$$

$$F_i^d \phi(r,t) - \lambda_i C_i(r,t) = \frac{\partial C_i(\bar{r},t)}{\partial t} \quad (i = 1,6)$$

in the usual notation.

These equations are solved either with spatial finite differences and the improved quasistatic (IQS) model in the CERBERUS code or with the modal expansion method utilized in the SMOKIN code.  Time-dependent cross sections representing the coolant-voiding transient, fuel temperature transient, reactor control system action, and shutoff rod movement are the driving functions for the neutron flux transient.  The space-dependence of coolant void produces a flux tilt in the horizontal direction, and shutoff rod insertion (SDS1) results in a major depression in the central region of the reactor core.  These tilts are represented qualitatively in Figure 9.1. The average power transient for the reactor is extracted from the calculation along with peaking factors for the average channel and the hot element in the loop being analyzed.  The system reactivity as a function of importance - weighted void fraction also is calculated.  These data are used as input to the thermal-hydraulics code SOPHT.  This code calculates the distribution of coolant void as a function of time from the pipe break, for each pass of the coolant loop.  The importance-weighted average void fraction calculated by SOPHT is combined with the pre-calculated reactivity function, and the average reactor power then are recalculated using a point kinetics model.  Peaking factors are applied to the average power transient as appropriate for each channel being modeled by SOPHT.  Fission product decay power is added to the neutron power.

Typical neutron power transients are shown in Figure 9.2. The decay power shown in Figure 9.3 is fitted to a sum of three exponential terms.
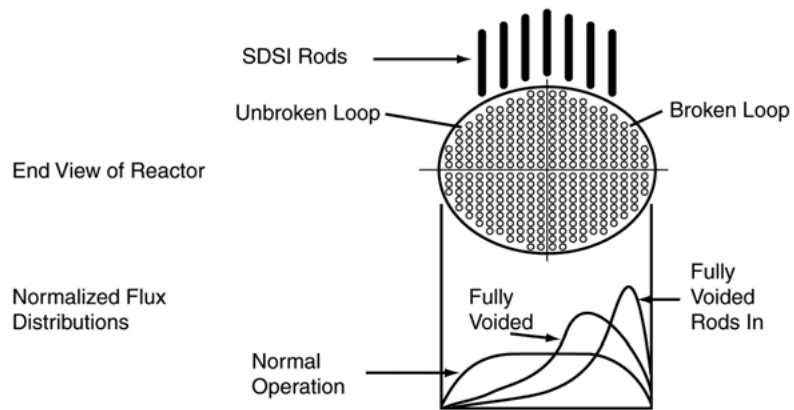
**FIGURE 9.1**
**SPATIAL POWER TRANSIENT DUE TO ONE-LOOP VOIDING**
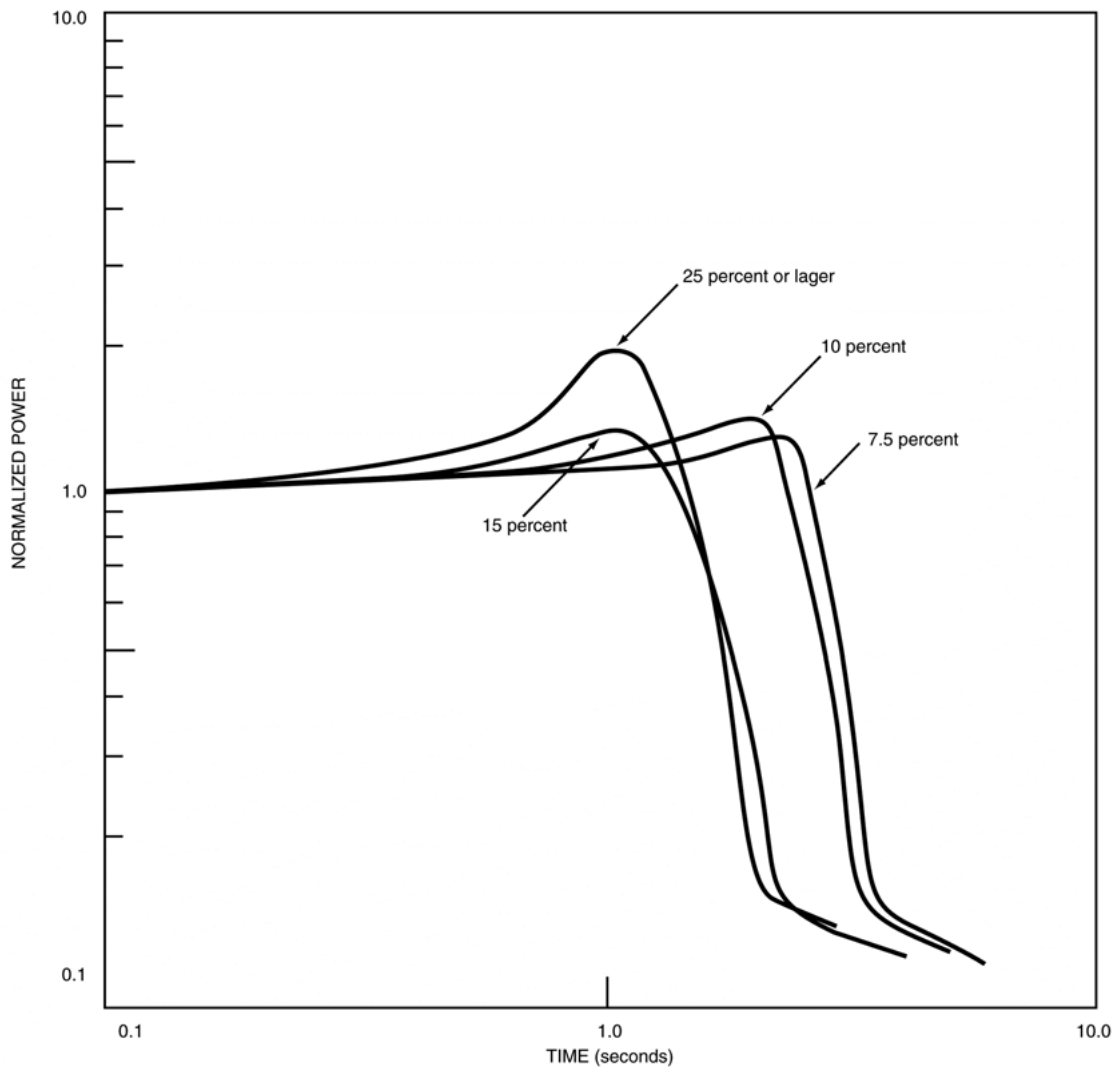
PPI649 9-1

**FIGURE 9.2
HOT ELEMENT POWER TRANSIENTS FOR
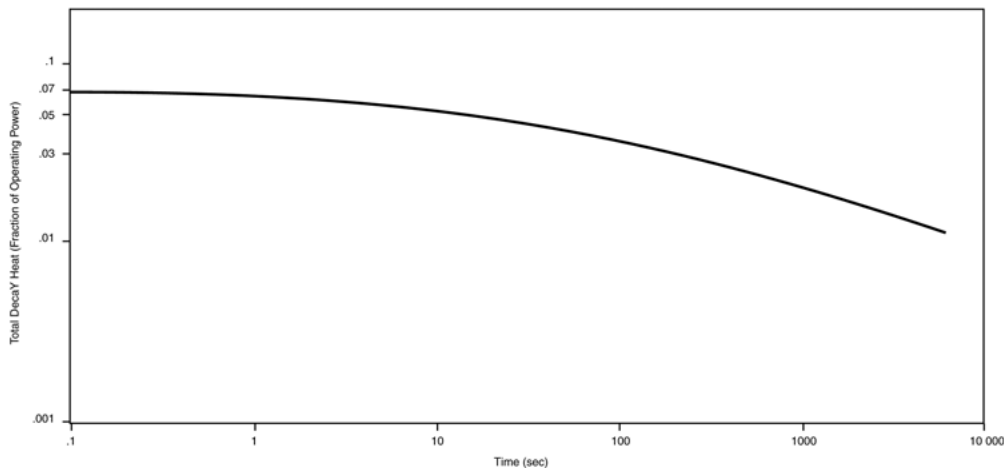REACTOR INLET HEADER BREAKS**

**FIGURE 9.3
DECAY POWER**

Fuel and Fuel Channel Behavior

Figures 9.4 to 9.12 summarize the behavior of fuel channels following a large LOCA. Channels are grouped into three categories (Fig. 9.4) depending on the amount of stored heat removed during blowdown. Typical values are shown in Fig. 9.5. The time-dependent temperature behavior of these three groups is shown in Fig. 9.6; blowdown may be followed by a prolonged stagnation period that is terminated by channel refill and rewet. Pressure tube ballooning (high internal pressure) or sagging (low internal pressure) takes place sometime during the blowdown/stagnation period. The coolant starvation time (Fig. 9.7) is determined by the calculated steam flow in the channel. Radial heat transfer models for normal, sagged, and ballooned channels are shown in Fig. 9.8; the axial geometry of a ballooned channel is shown in Fig. 9.9. The elements of the channel heat transfer model are shown in Fig. 9.10; typical results as a function of time (9.11) and axial channel position (9.12) indicate the characteristics of a steam-cooled channel prior to refill by the emergency injection system. Figures 9.13 to 9.15 show total fission product inventories, release characteristics, and typical release fractions calculated for a major LOCA in Bruce B.

---

**EARLY HEAT-UP:** THIS TYPE OF BEHAVIOR RESULTS FROM EARLY STAGNATION OF THE COOLANT FLOW. FOLLOWED BY A PROLONGED PERIOD OF COOLING BY A LOW STEAM FLOW. LITTLE OF THE FUEL STORED HEAT IS REMOVED DURING THE RAPID VOIDING OF THE CHANNELS, AND THE TEMPERATURE OF THE FUEL SHEATHS AND PRESSURE TUBE RISE RAPIDLY. EARLY FUEL FAILURES MAY OCCUR, AND THE HOT PRESSURE TUBE MAY STRAIN DIAMETRICALLY TO CONTACT ITS CALANDRIA TUBE. THIS LATTER PHENOMENON IS REFERRED TO AS PRESSURE TUBE BALLOONING.

---

**DELAYED HEAT-UP:** THE FUEL STORED ENERGY IS PARTIALLY REMOVED BY LIQUID AND TWO-PHASE COOLANT PRIOR TO THE ONSET OF A PROLONGED STEAM COOLING PERIOD, RESULTING IN A SLOWER HEAT-UP WITHIN THE CHANNEL RELATIVE TO THE EARLY HEAT-UP CHANNELS. BY THE TIME THE PRESSURE TUBE TEMPERATURE RISES SIGNIFICANTLY, THE SYSTEM PRESSURE IS SUFFICIENTLY LOW SUCH THAT ONLY ASYMETRIC PRESSURE-TUBE/CALANDRIA TUBE CONTACT OCCURS, BY A COMBINATION OF PRESSURE-TUBE SAGGING AND BALLOONING.

**LATE HEAT-UP:** MOST OF THE FUEL STORED IS REMOVED PRIOR TO THE ONSET OF STEAM COOLING, AND HEAT-UP BEGINS FROM FUEL AND PRESSURE TUBE TEMPERATURES NEAR COOLANT SATURATION TEMPERATURE. TEMPERATURES INCREASE VERY SLOWLY RELATIVE TO CATEGORIES (A) AND (B), AND ANY PRESSURE TUBE DEFORMATION WILL BE BY SAGGING ONLY.

**Figure 9.4 – Characterization of behaviour of fuel channels under different post-LOCA conditions**
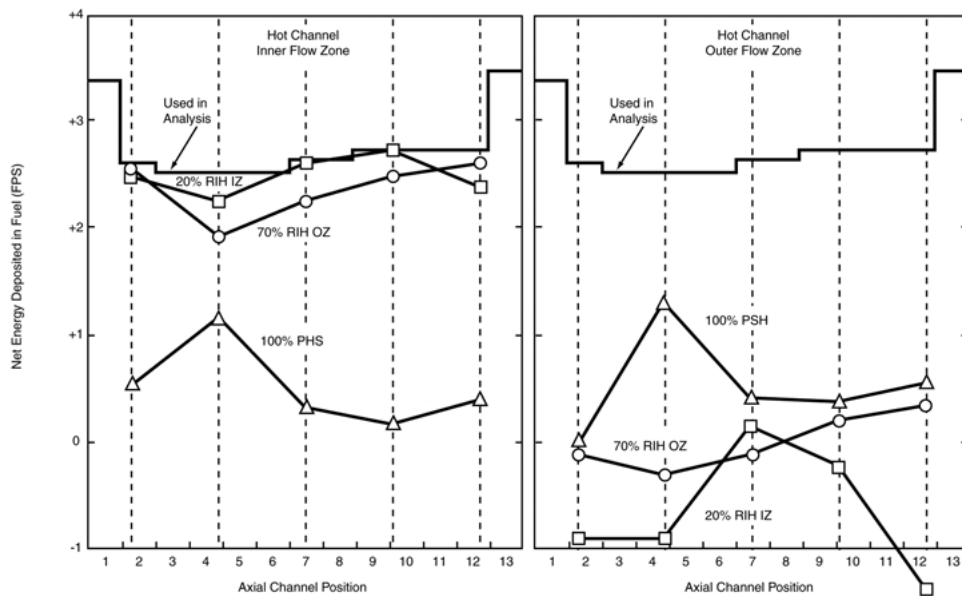


FIGURE 9.5
NET ENERGY DEPOSITED IN HOT CHANNEL DURING CHANNEL VOIDING PERIOD

PPI649 9-5
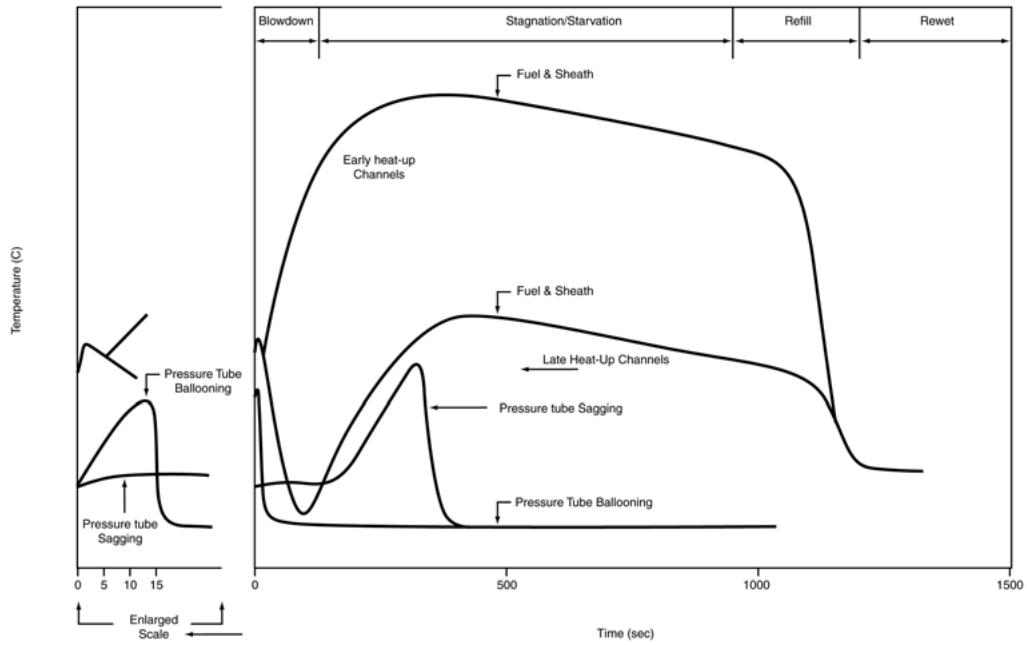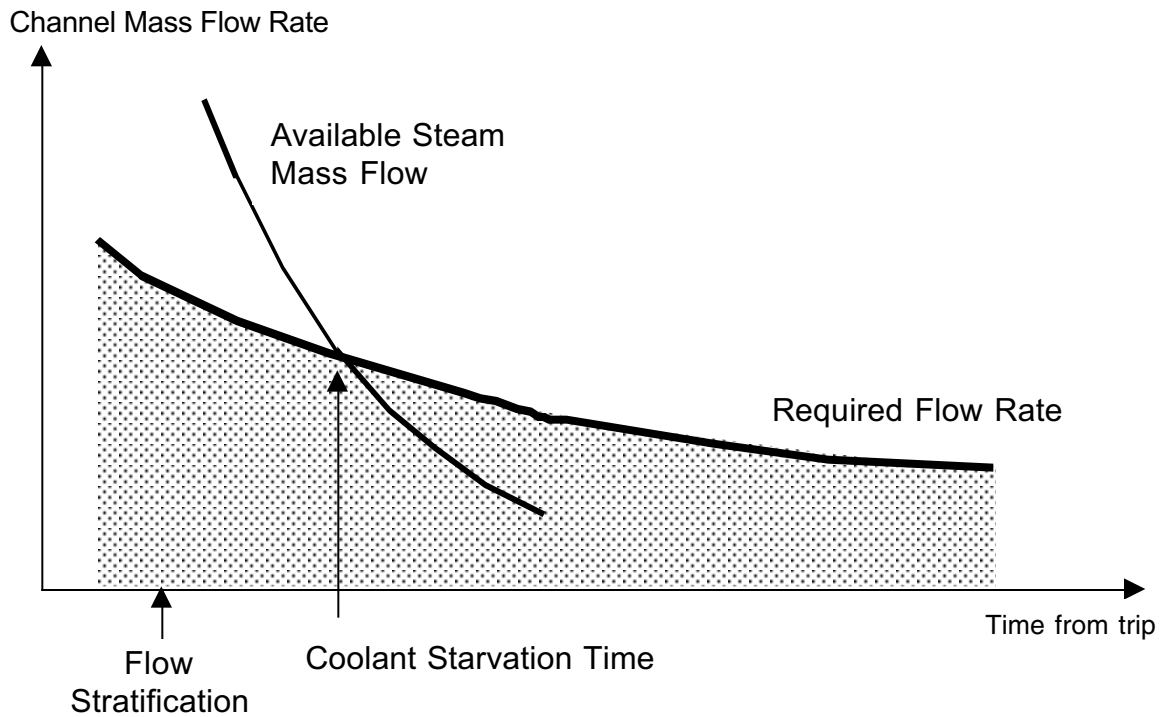
**FIGURE 9.6**
**FUEL CHANNEL CHARACTERIZATION**

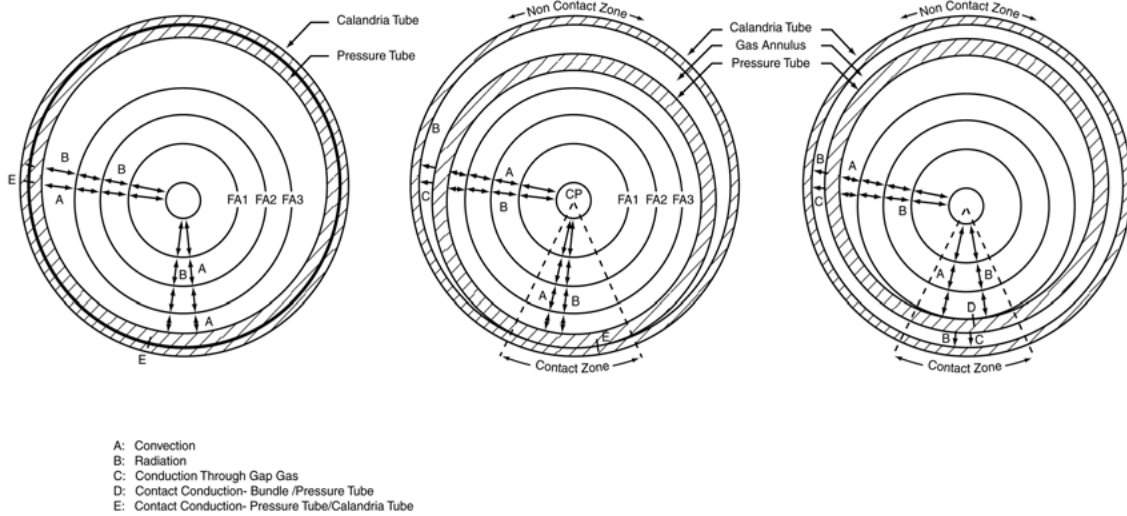PPI649 9-6



**FIGURE 9.7 -- CALCULATION OF COOLANT STARVATION TIME**

A: Convection
B: Radiation
C: Conduction Through Gap Gas
D: Contact Conduction- Bundle /Pressure Tube
E: Contact Conduction- Pressure Tube/Calandria Tube

**FIGURE 9.8**
**Models for Deformed Fuel Channel Segment**

Calandria Tube
Pressure Tube

Non Contact Zone
Calandria Tube
Gas Annulus
Pressure Tube

Non Contact Zone

Contact Zone

Contact Zone

Increased
Area for
Flow

When internally pressurized Zr-2.5%Nb
pressure tubes are exposed to the type
of temperature excursions that
occur during postulated loss of coolant /
loss of emergency core cooling transients
they may strain into contact with the
calandria tube

Ballooned Pressure Tube

Unstrained Bundle

No Calandria Tube
Strain

No Strain
or Partial
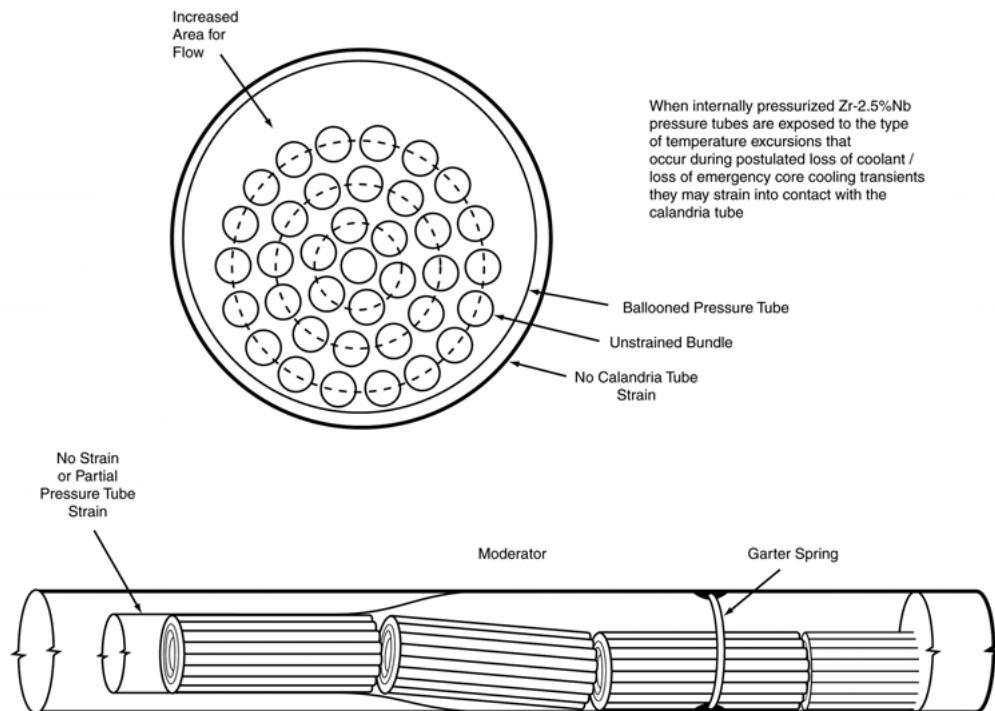Pressure Tube
Strain

Moderator

Garter Spring

**FIGURE 9.9**
**PRESSURE TUBE DIAMETRAL STRAIN TO CONTACT**
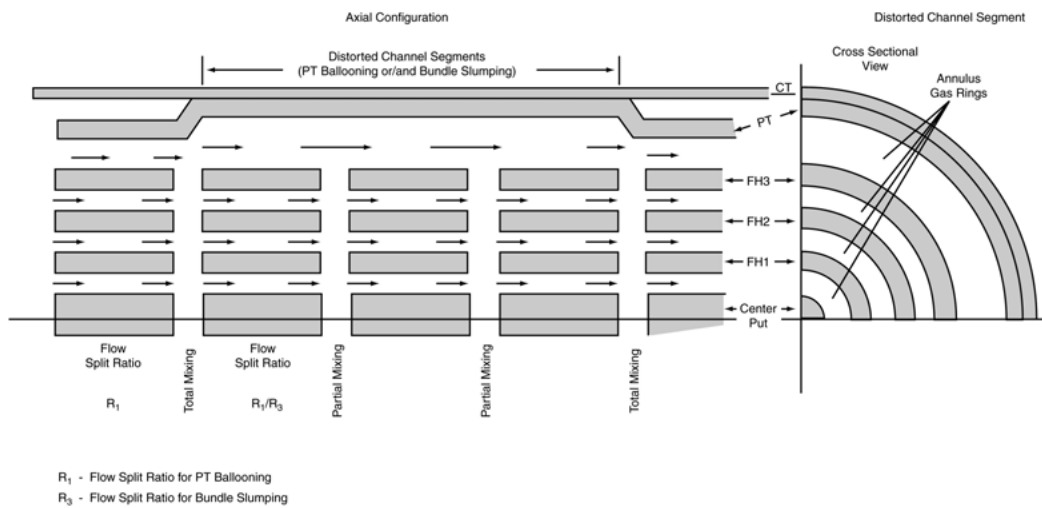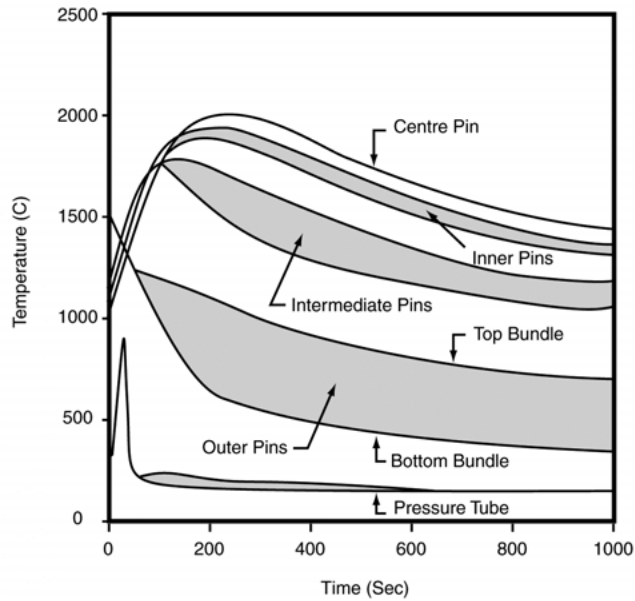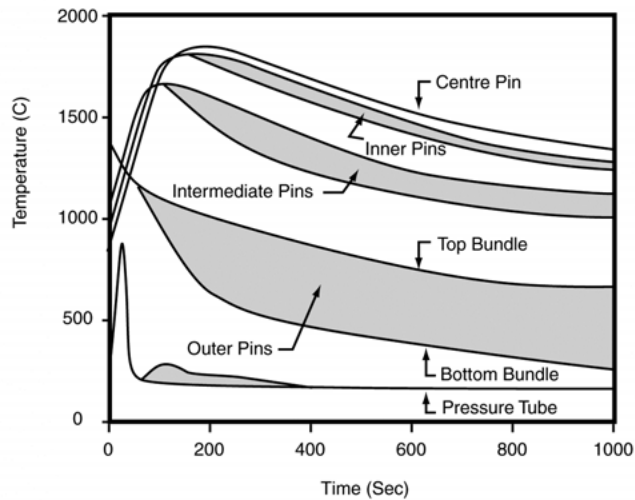
*Rev. 1,  Oct. 2003*

**FIGURE 9.10**
**FLOW REDISTRIBUTION AND MIXING MODEL**

**Temperature transients at hottest bundle position (No.8) in early heatup 7.5 MW channel (Channel voided at 5s. superheated steam flow of 100 g/s thereafter)**



**Temperature transients at hottest bundle position (No.8) in early heatup 6.7 MW channel (Channel voided at 5s. superheated steam flow of 100 g/s thereafter)**
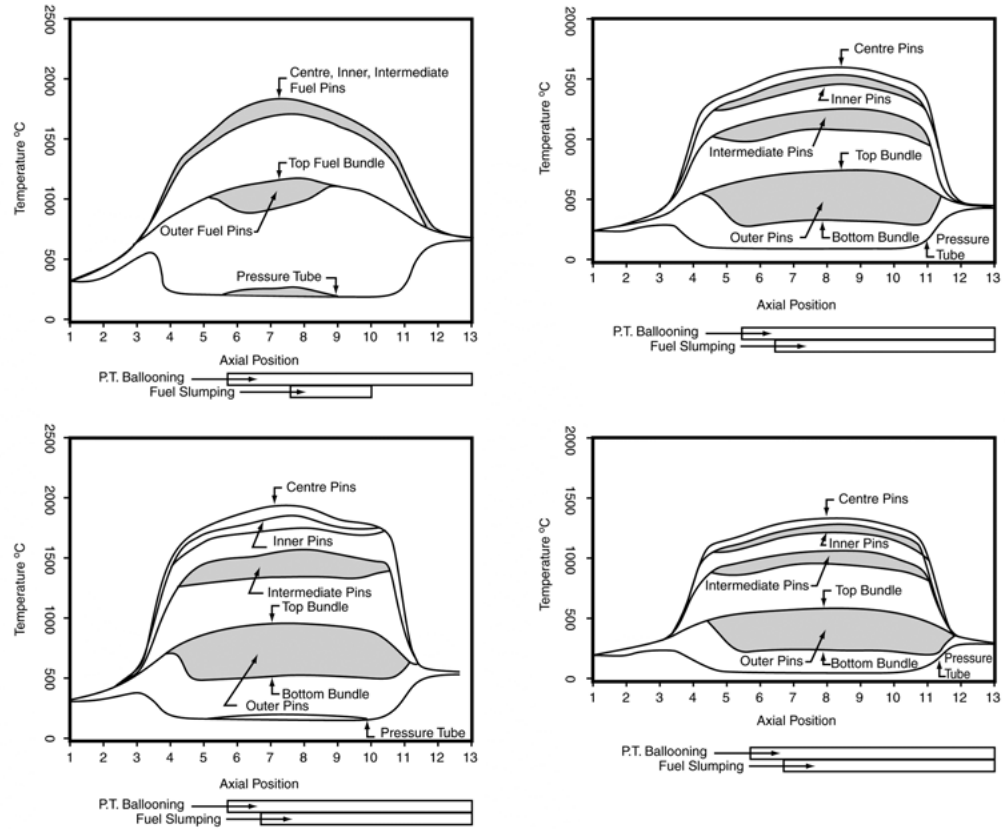
**FIGURE 9.11**

**FIGURE 9.12**
**TEMPERATURE PROFILES IN EARLY HEATUP 7.5 MW CHANNEL**
**(CHANNEL VOIDS AT 5s, SUPERHEATED STEAM FLOW OF 100g/s THEREAFTER**

ᴾPI649 9-12

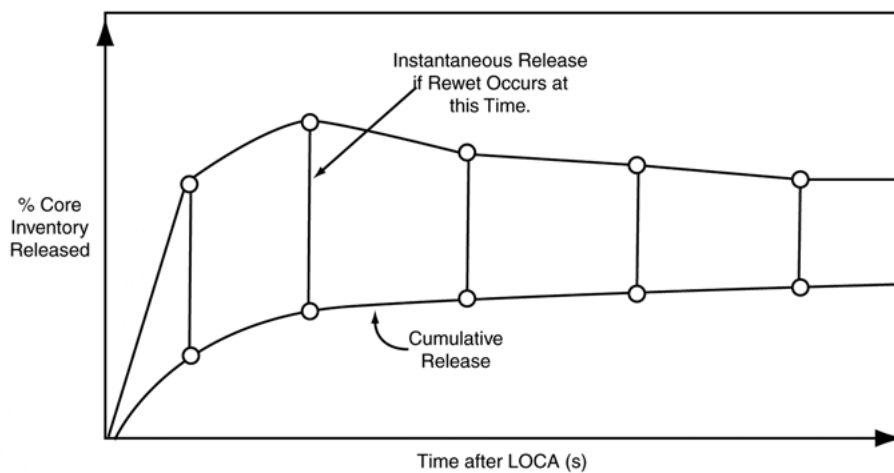**FIGURE 9.13**
**Core Grain Boundary and Free Inventory Fractions**

| Fission Product Group | Governing Isotope of Group (a) | | | | Distribution (% Core Inventory) (b) | | | | | |
|---|---|---|---|---|---|---|---|---|---|---|
| | | | | | Nominal Core | | | SHIM Core | | |
| Species | Half Life Range | Isotope | Half Life | Total Core Inventory | Grain Boundary Inventory ((GB) | Free Inventory | GB & Free | Grain Boundary (GB) | Free Inventory | GB & Free |
| Short Lived Noble Gasses | 1<10 h | Xe135 | 9.1 h | 34.0 EBq* (19.9 EBq t<3min) | 0.04 | 0.004 | 0.044 | 0.10 | 0.04 | 0.14 |
| Intermediate Lived Noble Gasses | 10 h<1<20 d | Xe133 | 5.3 d | 6.8 EBq | 0.89 | 0.04 | 0.73 | 1.62 | 0.55 | 2.17 |
| Long Lived Noble Gasses | 1>20 d | Kr85 | 11 y | 6.1 PBq** | 9.58 | 0.30 | 9.88 | 10.72 | 1.92 | 12.64 |
| Short Lived Halogens | 1<10 h | M35 | 6.6 h | 29.9EBq | 0.03 | 0.02 | 0.05 | 0.07 | 0.11 | 0.18 |
| Intermediate Lived Halogens | 10 h<1<10 d | M31 | 8.0 d | 13.4 EBq (29.9 EBq 1-131) | 0.72 | 0.35 | 1.07 | 1.23 | 1.58 | 2.81 |
| Long Lived Alkali Metals | 1>20 d | Cs137 | 30 y | 0.1 EBq | 7.62 | 2.24 | 9.86 | 7.46 | 5.14 | 12.60 |
| Intermediate Lived Chalogens | 10 h<1<10 d | Te132 | 3.3 d | 4.7 EBq | 0.32 | 0.16 | 0.48 | 0.65 | 0.92 | 1.57 |
| Long Lived Alkaline Earths Rare Earths Noble metals, etc | 1>20 d | Sr80 | 50.5 d | 15.2 EBq | n/a | 0.02 | 0.02 | n/a | 0.08 | 0.08 |

Notes:
(a) Isotope with highest fractional Inventory (on core basis) from a number of species examined.
(b) All Isotopes of the group are assumed to have this fractional invantory, although most of them will have a lower fraction.

(*) 1EBq=$10^{15}$ Bq
(**) 1PBq=$10^{15}$ Bq

200649 9-13

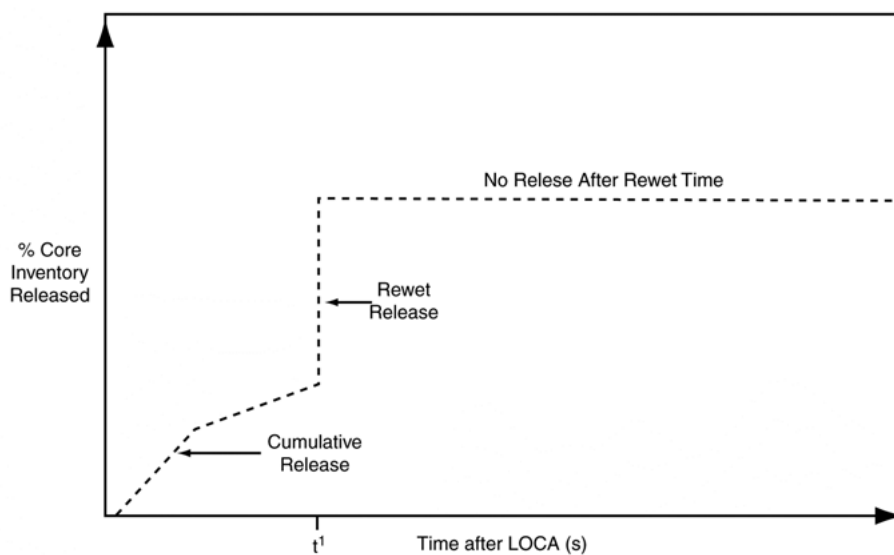**GENERIC CURVE OF FISSION PRODUCT RELEASE FROM FUEL INTO CORE**



**FIGURE 9.14**
**AN EXAMPLEOF FISSION PRODUCT RELEASE INTO THE CORE**
**ASSUMING REWET @ TIME.t**

PPI649 9-14

| | Fission Product Group | Total Release During Accident (% Core Inventory) | Ultimate Release (% Core Inventory) |
|---|---|---|---|
| Equilibrium Core in SHIM Mode of Operation | Noble Gas (t≤10 h)* | 0.57 | 1.01 |
| | Noble Gas (10 h<t<20 d) | 1.15 | 1.59 |
| | Noble Gas (t≥20 d) | 2.37 | 2.81 |
| | Halogens (t≤10 h) | 0.86 | 1.30 |
| | Halogens (10 h<t<10 d) | 1.63 | 2.07 |
| | Long lived Alkali Metals | 3.75 | 4.19 |
| | Intermediate Lived Chalcogens | 1.29 | 1.73 |
| | Long Lived Alkaline Earths | 1.37 | 1.81 |
| Pre-Equalibrium Core in NOMINAL Mode of Operation | Noble Gas (t≤10 h) | 0.16 | 0.67 |
| | Noble Gas (10 h<t<20 d) | 0.28 | 0.79 |
| | Noble Gas (t≥20 d) | 1.00 | 1.51 |
| | Halogens (t≤10 h) | 0.20 | 0.71 |
| | Halogens (10 h<t<10 d) | 0.52 | 1.03 |
| | Long lived Alkali Metals | 2.12 | 2.63 |
| | Intermediate Lived Chalcogens | 0.35 | 0.86 |
| | Long Lived Alkaline Earths | 0.38 | 0.89 |
| Equalibrium Core in NOMINAL Mode of Operation | Noble Gas (t≤10 h)* | 0.10 | 0.60 |
| | Noble Gas (10 h<t<20 d) | 0.16 | 0.66 |
| | Noble Gas (t≥20 d) | 0.68 | 1.18 |
| | Halogens (t≤10 h) | 0.12 | 0.62 |
| | Halogens (10 h<t<10 d) | 0.30 | 0.80 |
| | Long lived Alkali Metals | 1.48 | 1.98 |
| | Intermediate Lived Chalcogens | 0.20 | 0.70 |
| | Long Lived Alkaline Earths | 0.22 | 0.72 |

*t= half-life

**FIGURE 9.15**
**LONG-TERM ACTIVITY RELEASE FROM THE FUEL FOR A LARGE BREAK LOCA**

PPI649 9-15

## Moderator Thermal-Hydraulics

When pressure tubes contact calandria tubes, either by ballooning or sagging, the heat transfer rate to the moderator increases abruptly.  If this heat flux exceeds the critical heat flux for that channel, the calandria tube will dry out.  Since the post-dryout heat transfer coefficient is very low, the calandria tube would be effectively insulated on its outer surface, so its temperature would increase rapidly.  This picture must be modified by the recognition that the pressure tube

contact may be local, particularly for sagging contact.  Radial and axial heat transfer through the calandria tube would tend to control its temperature; in addition, the boiling water on the outer surface would produce buoyancy flow that would promote cooling.  Experiments have shown that calandria tubes do not remain dry for an extended period, even when the initial heat flux on contact is well beyond the dryout level.  Nevertheless, for purposes of licensing, dryout has been taken to be the safety limit.  Figure 9.16 shows the results of dryout experiments in simulated full-scale fuel channels.  The key question is: what is the maximum permitted temperature in the surrounding moderator water before contact, such that dryout will not occur?  (The critical heat flux decreases as the amount of pre-contact subcooling decreases).  It can be seen from Fig. 9.16 that the subcooling required to prevent dryout increases with contact temperature and decreases with the contact pressure between pressure tube and calandria tube.  These effects indicate that there must be an upper limit to the required subcooling, because (a) the pressure tube cannot be heated at a rate higher than adiabatic, (b) sagging or ballooning will occur when a certain temperature is reached, and (c) higher temperature at contact accompanies lower internal and therefore lower contact pressure.  The maximum contact temperatures are plotted in Figure 9.17.
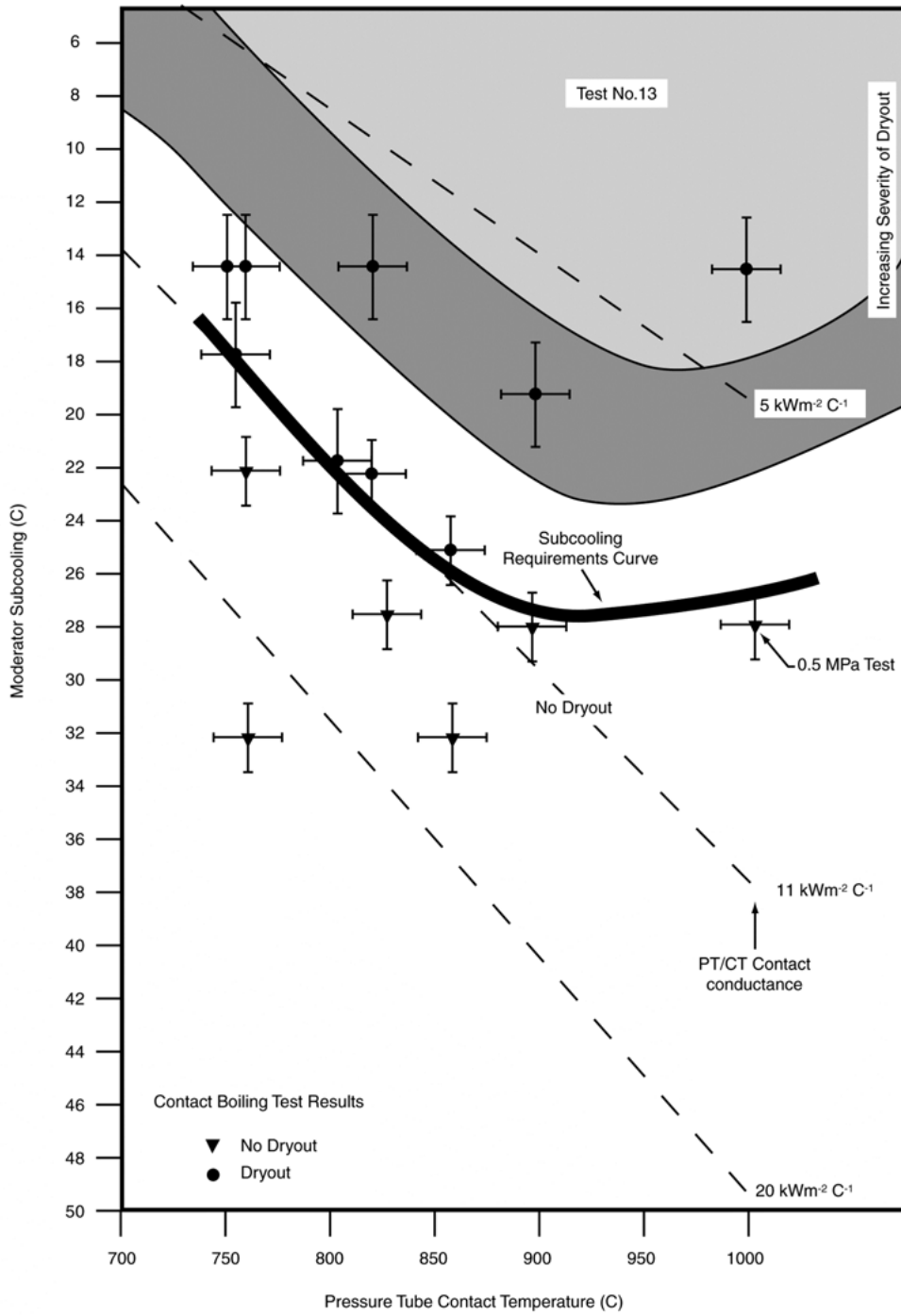
**FIGURE 9.16**
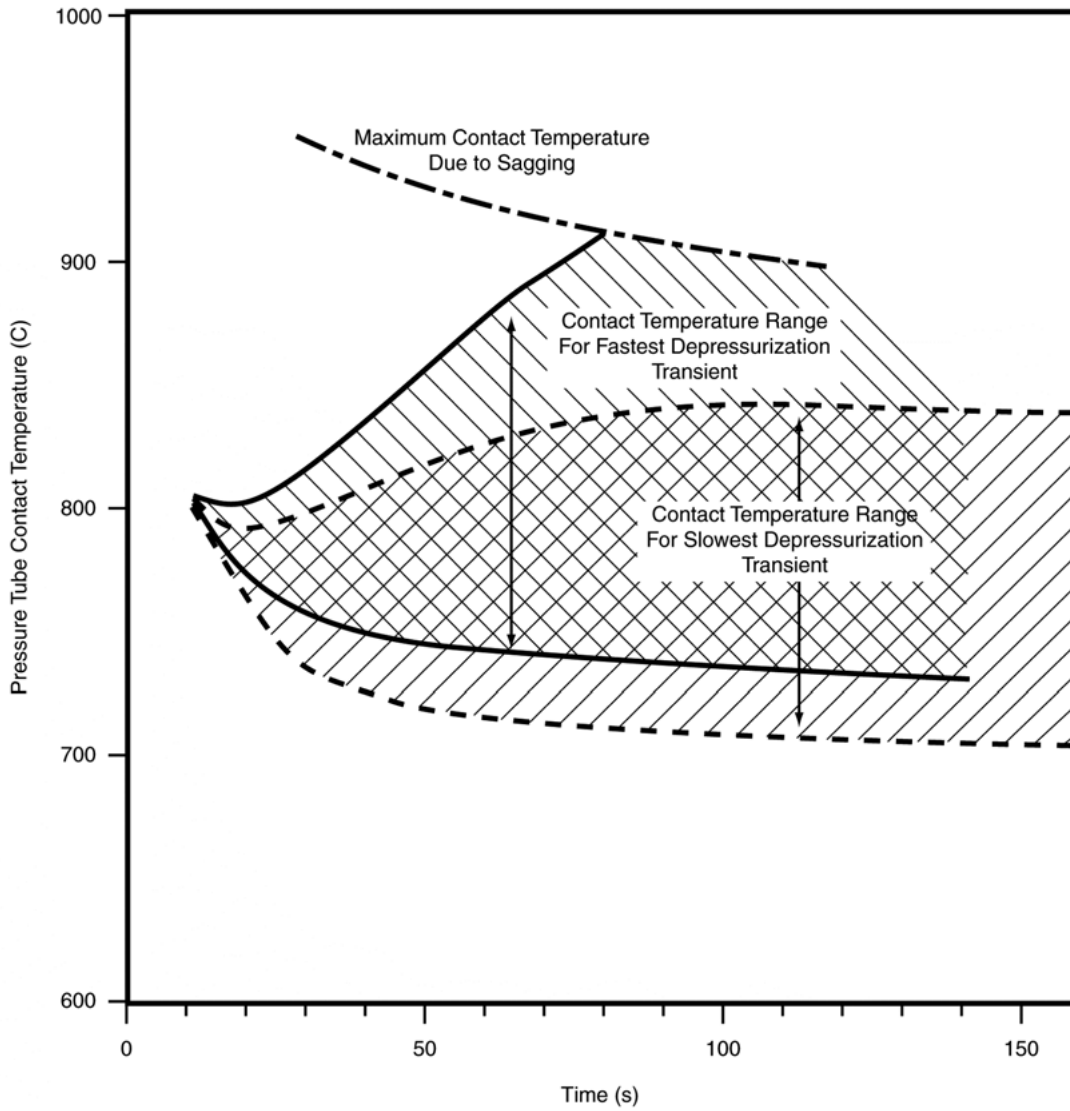**CALANDRIA TUBE DRYOUT CURVE**

PPI649 9-16

**FIGURE 9.17**
**PRESSURE TUBE CONTACT TEMPERATURE**

PPI649 9-17

The local temperature of the moderator water is determined mainly by the inlet temperature, the pre-accident heat deposition rate (via neutron and gamma bombardment), the power rundown after the LOCA, and the flow pattern inside the calandria tank. Figure 9.18 shows the configuration of the calandria heat removal system. Nozzles on each side of the tank direct flow upwards and toward the center; the outlet flow is taken from the bottom of the tank.

A typical calculated flow pattern is shown in Figure 9.19.  These calculated temperatures are modified by the static head on the particular channel in question (static head affects saturation temperature) to arrive at a figure for the minimum available subcooling. Figure 9.20 shows a typical resultant subcooling margin as a function of time after LOCA.  The allowable maximum calandria outlet temperature, moderator flow, and therefore the pumping power required for moderator cooling are determined by this margin.
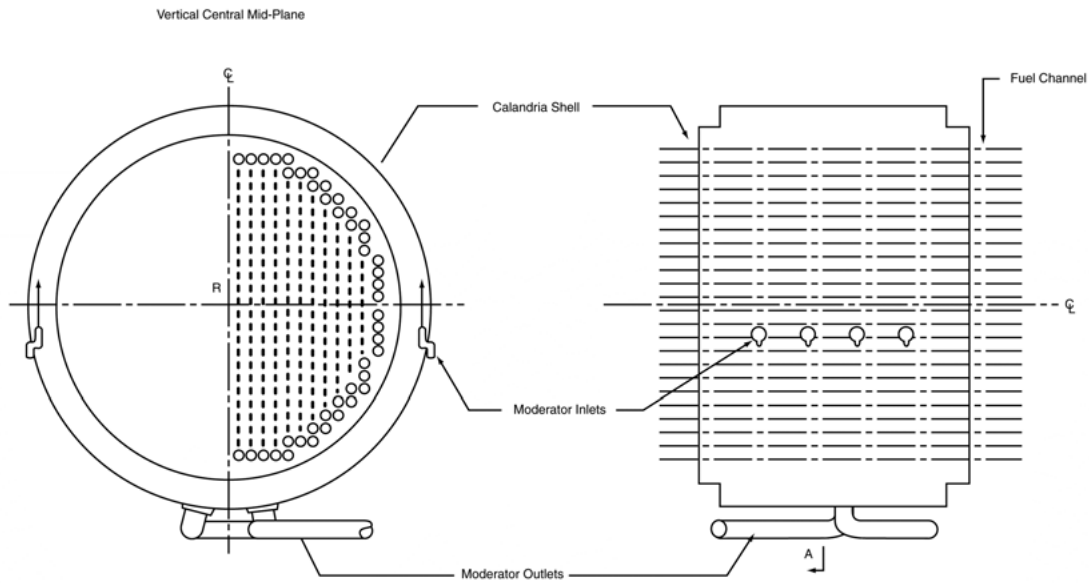


**FIGURE 9.18**
**END AND SIDE VIEWS OF CALANDRIA VESSEL**
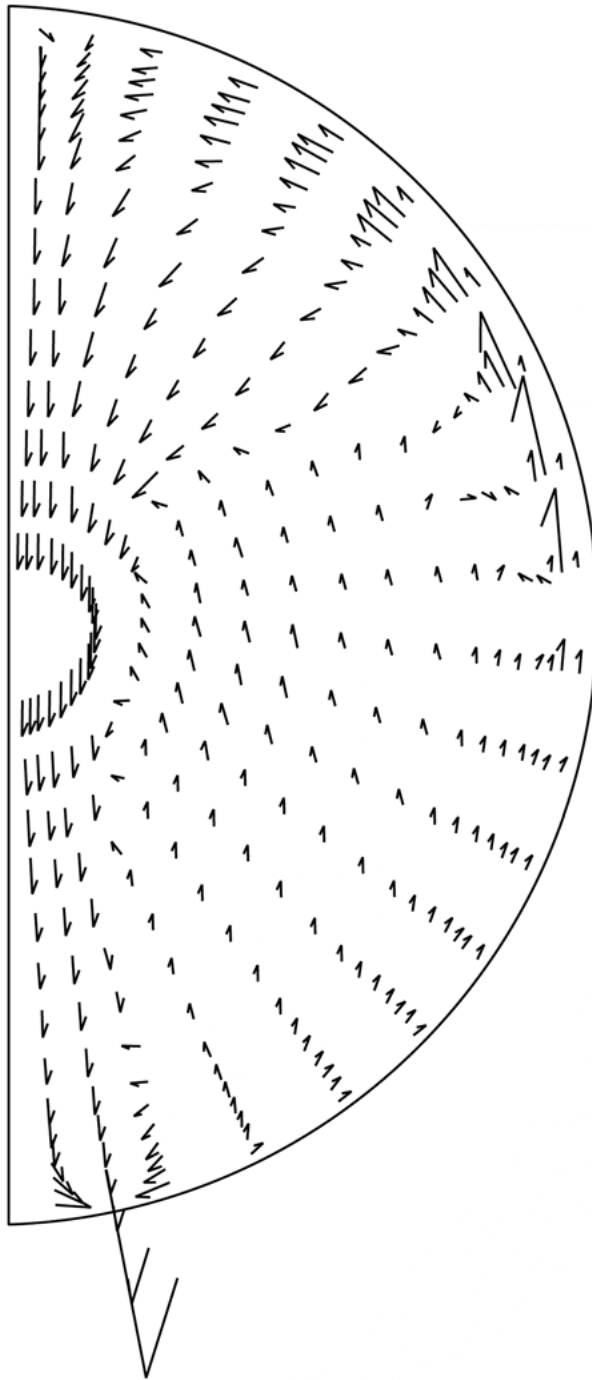
ᴾPI649 9-18

**FIGURE 9.19**
**FLOW PATTERN IN THE R-O PLANE (Z=2.925 m)**
**AT 100 PERCENT FULL POWER STEADY RATE**
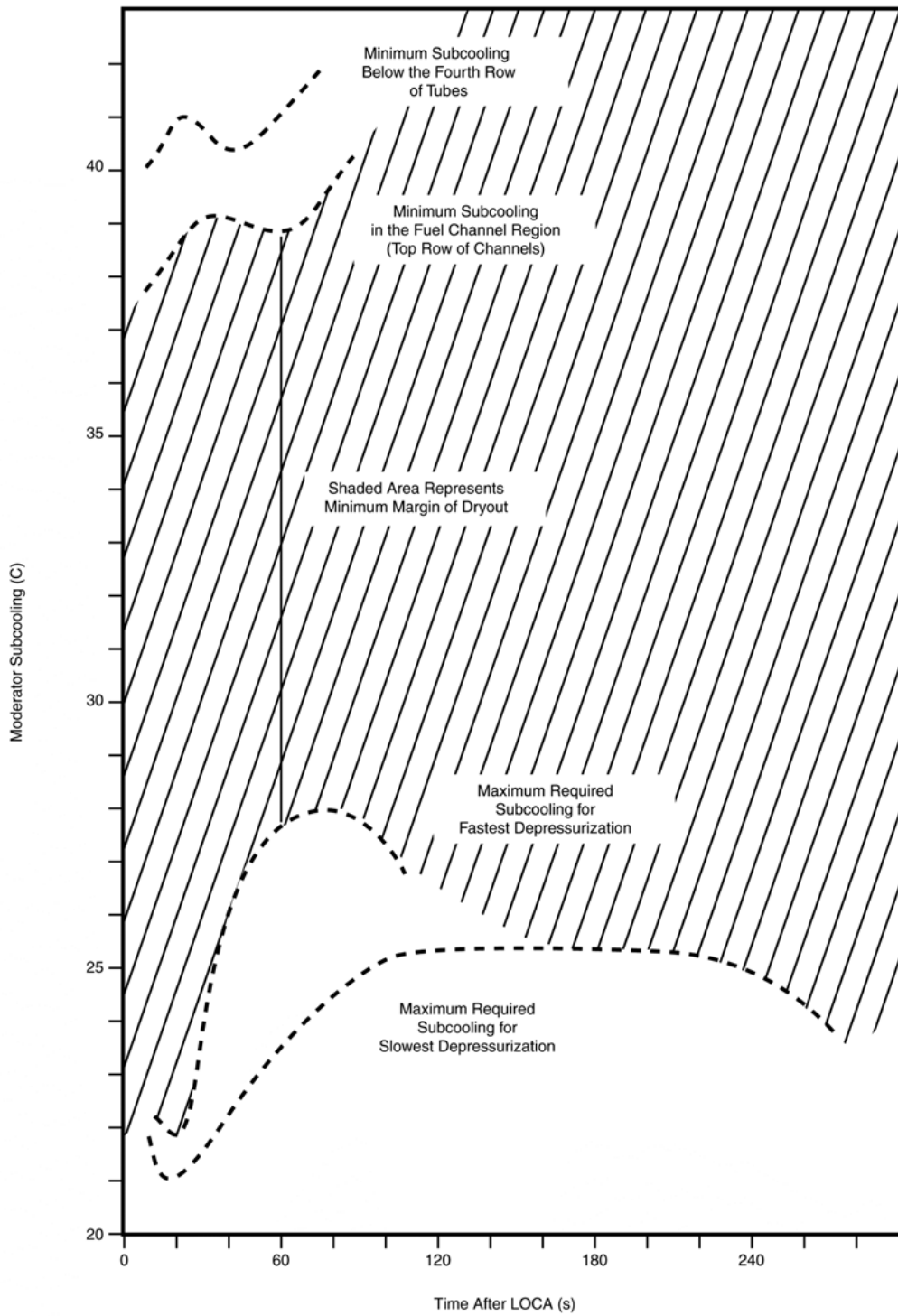
PPI649 9-19

**FIGURE 9.20**
**MAXIMUM MODERATOR SUBCOOLING REQUIREMENTS FOLLOWING A LOCA**

PPI649 9-20

Containment Response

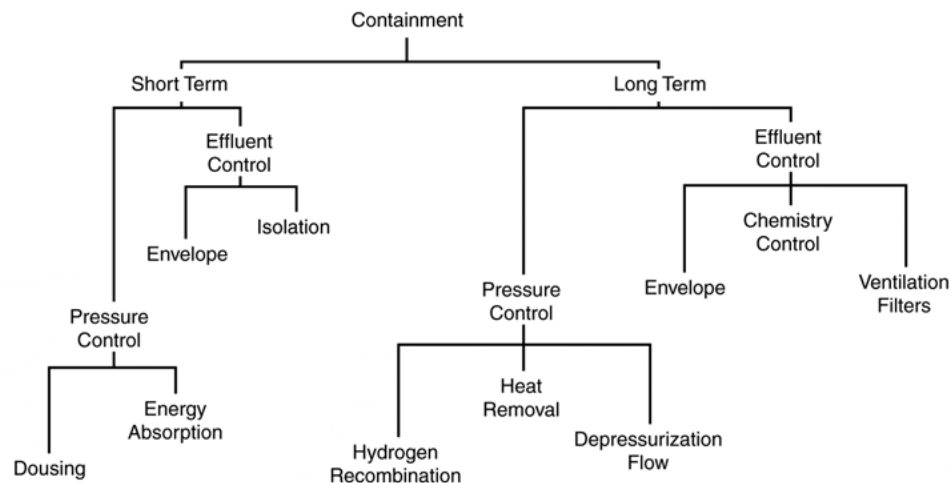Required containment functions are:
(a) Normal Operation
- protect reactor and equipment from external elements (keep the rain off).
- provide a well-defined access control barrier for operating staff.
- protect against external accident initiating events (e.g. blast, wind,
   aircraft crash, etc.).
- provide means for controlling and monitoring ventilation flows around systems
containing radioactive materials.
(b) Post-Accident
- The functions related to containment of radioactive materials released in an accident are
shown in Figure 9.21.



**FIGURE 9.21**
**POST-ACCIDENT CONTAINMENT FUNCTIONS**

PPI649 9-21

These containment functions can be accomplished in a number of different ways. Figures 9.22 to 9.25 show the major classes of containment systems now used in power reactors.

Referring back to Figure 9.21, in the 600 MW CANDU units short-term pressure control is accomplished by a pressure-actuated dousing system located at the top of the containment building. Redundant valves supply six sectors of dousing spray headers. Steam issuing from the HT break is condensed by the spray; its energy appears as sensible heat in the water on the building floor. Energy absorption by internal structures and containment walls is the second, inherent, means of short-term pressure control.

Short-term effluent control is supplied jointly by the building envelope and the isolation mechanisms on the building ventilation system.  Isolation usually is initiated by either high pressure or high radiation levels in the ventilation duct.

In the long term, pressure control is achieved by removing stored and decay heat from containment, by depressurization through filtered air discharge lines, and (if required) hydrogen recombination to preclude the possibility of a hydrogen fire with its consequent sudden release of heat energy.  (Figures 9.26 and 9.27 show the amount of hydrogen generated in LOCA scenarios with no emergency coolant injection, and typical peak overpressure values inside the vault.  Both figures are for Bruce B).
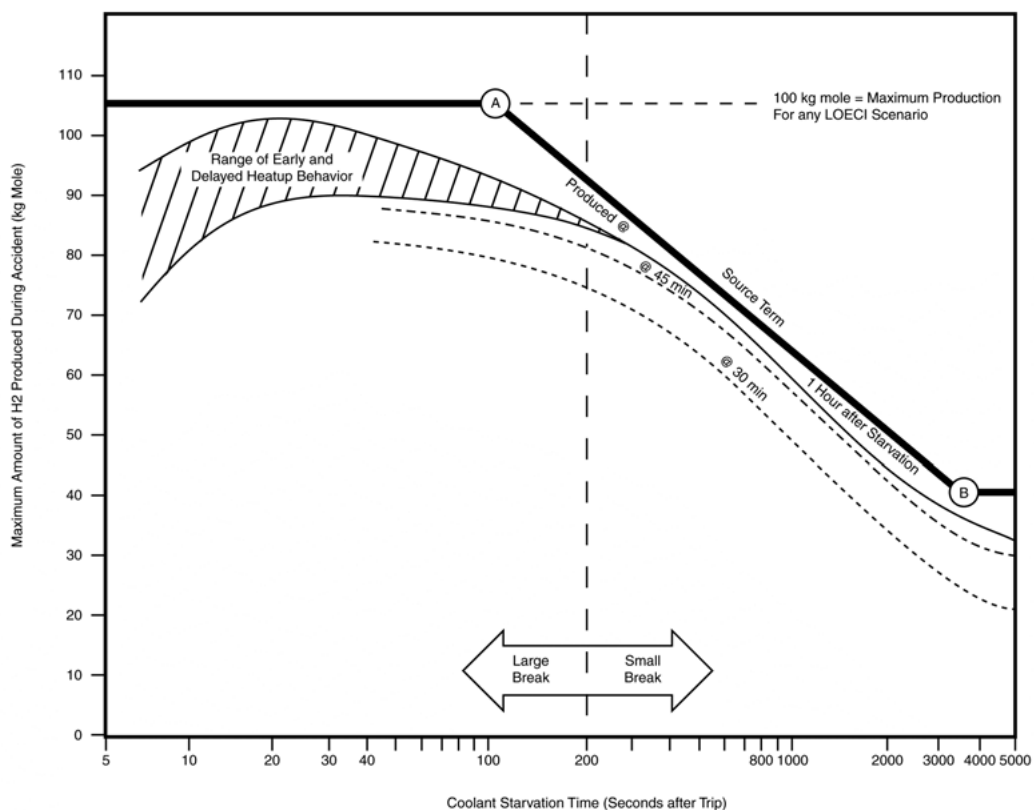


**FIGURE 9.26**
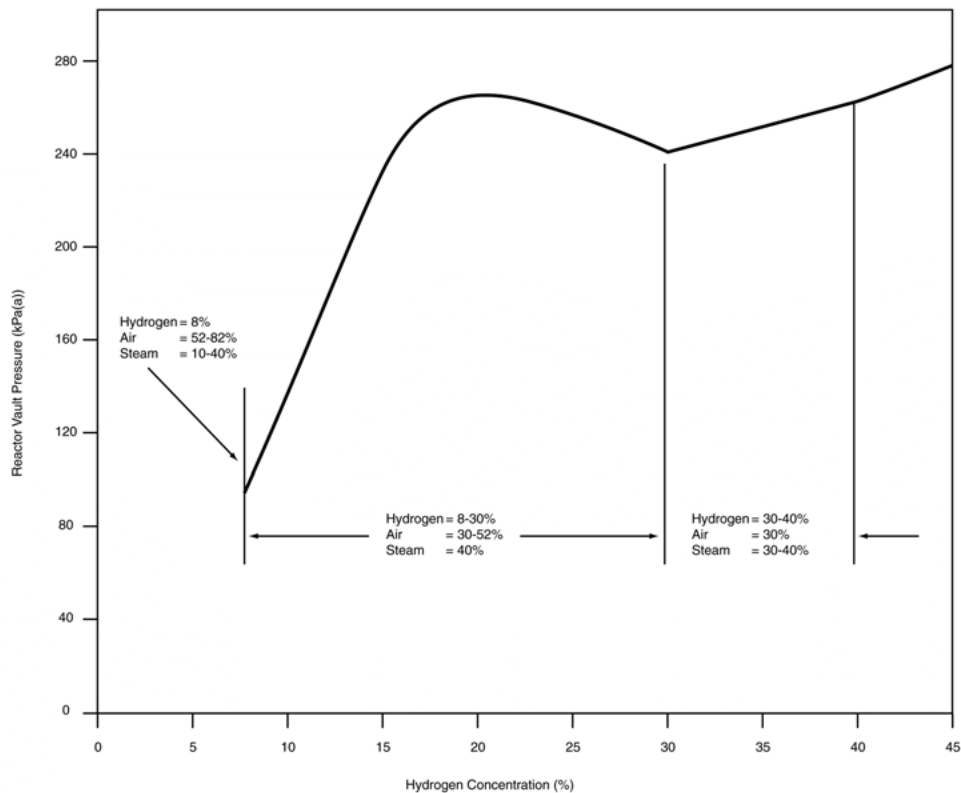**HYDROGEN PRODUCTION IN LOECI SCENARIOS**

PPI649 9-26

**FIGURE 9.27**
**PEAK PRESSURES IN REACTOR VAULT FOR RANGE OF HYDROGEN AIR STREAM**
**MIXTURES ALONG IGNITION CRITERION**

PPI649 9-27

Effluent control in the long term is achieved by the sealed containment envelope, by water chemistry control, and by the ventilation filters. Water chemistry control is important because the amount of some radioactive materials in the vapor phase (available for release during overpressure periods) is sensitive to the oxidation potential and pH of the water. Iodine-131 is the most important isotope in this group. Ventilation filters consist of high- efficiency particulate (HEPA) filters and activated charcoal beds in series. These filters are preceded by a ventilation drier and (usually) a preheater to ensure the air passing through the charcoal filter remains above the dewpoint temperature.

Typical short-term and long-term pressure transients in the CANDU 600 containment are shown in Figures 9.28 and 9.29. Heat sources and sinks, and typical post-accident energy balances, are shown in Figures 9.30 and 9.31.
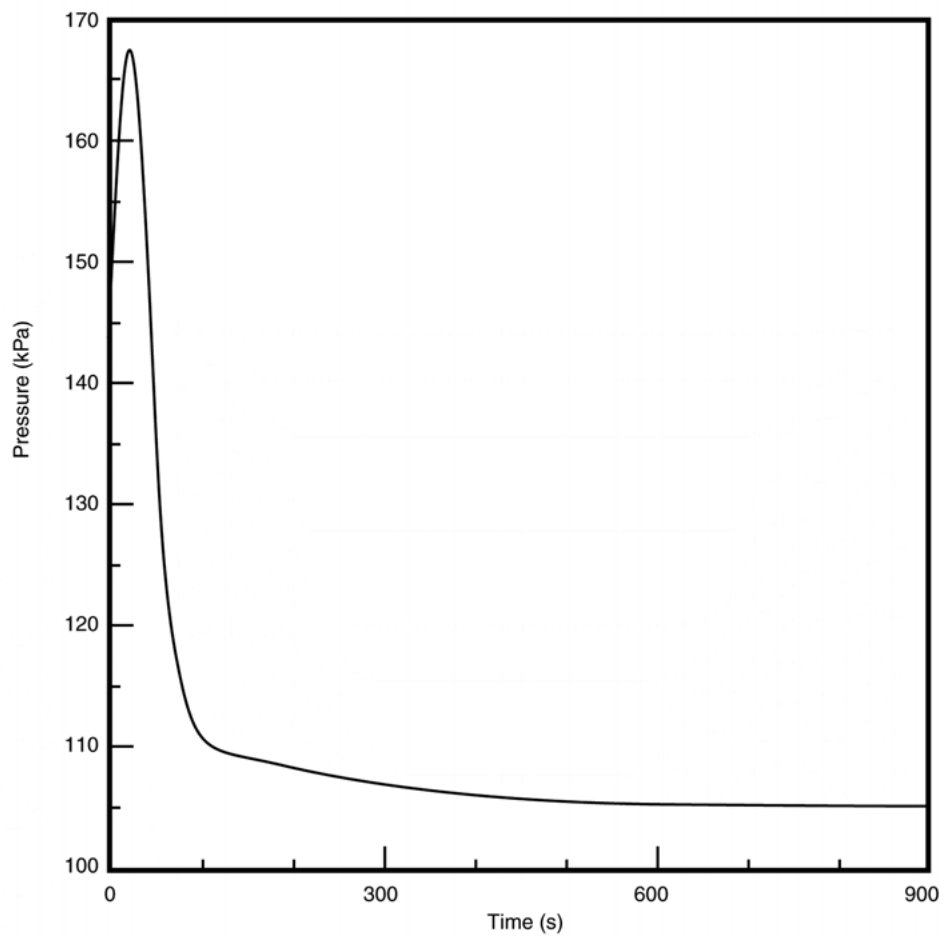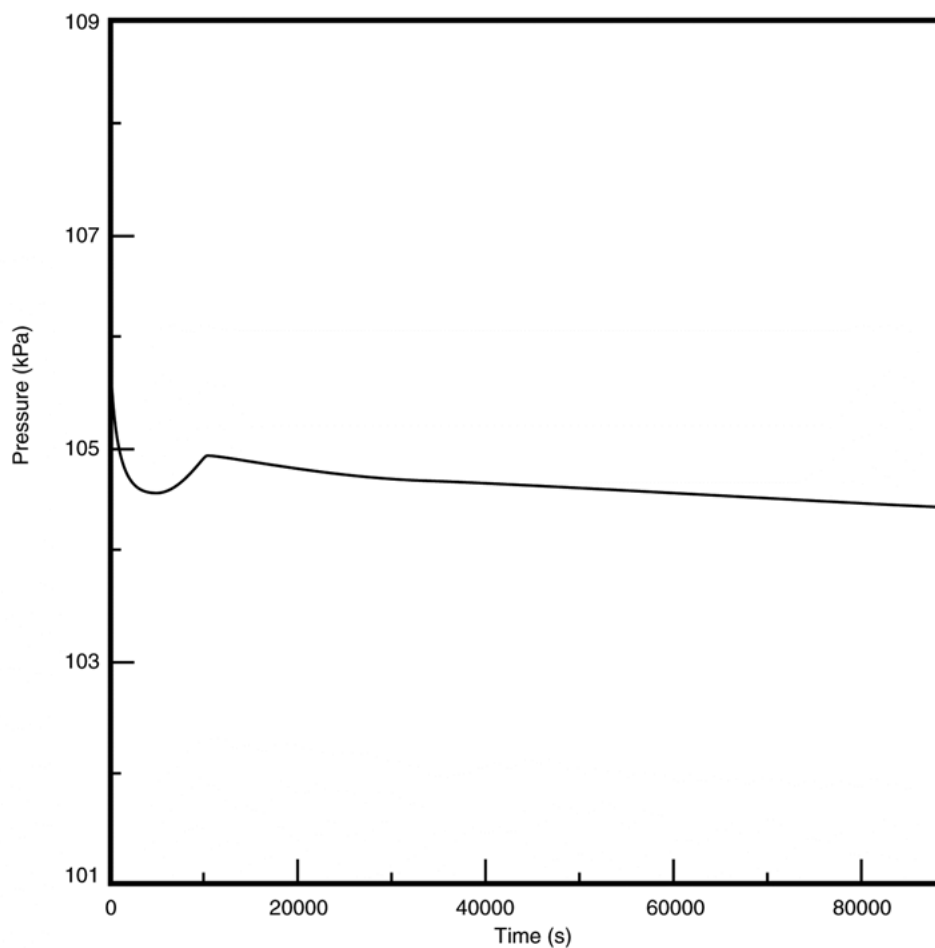
**FIGURE 9.28**
**SHORT TERM INTACT CONTAINMENT PRESSURE TRANSIENT**
**FOR 80 PERCENT REACTOR OUTLET HEADER BREAK**

PPI649 9-28

**FIGURE 9.29**
**INTACT CONTAINMENT PRESSURE TRANSIENT UP TO ONE DAY**
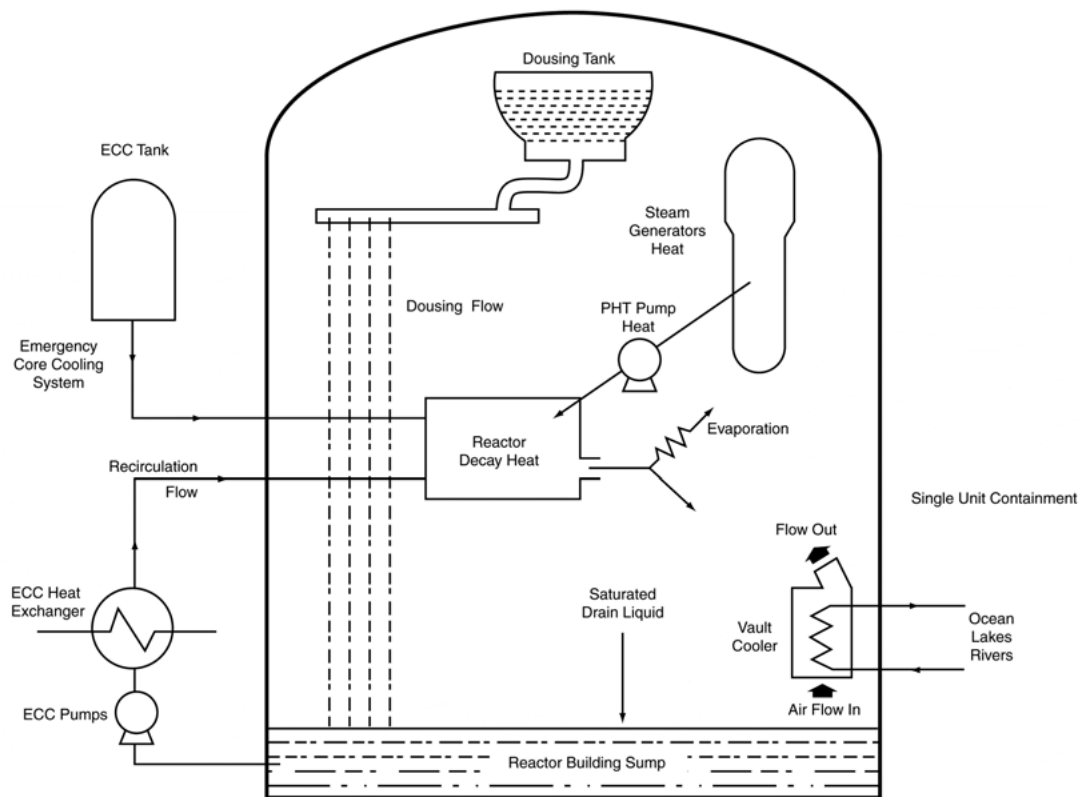**AFTER AN 80 PERCENT REACTOR OUTLET HEADER BREAK**

PPI649 9-29

*Rev. 1,  Oct. 2003*

**FIGURE 9.30**
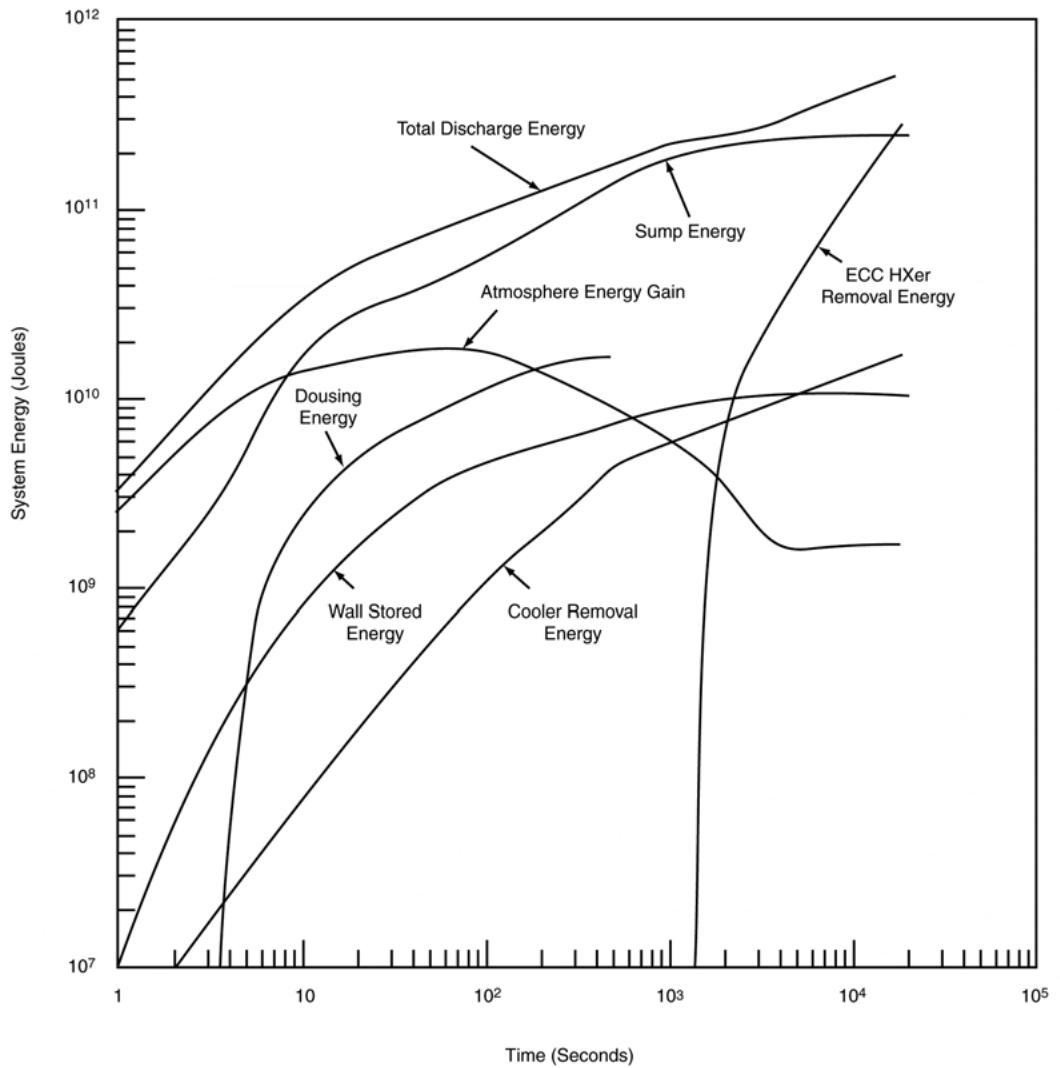**SCHEMATIC DIAGRAM OF RECIRCULATING CORE COOLING SYSTEM**

**FIGURE 9.31**
**LONG TERM CONTAINMENT ENERGY SOURCES AND SINKS**

Radioactivity Release from Containment

Figure 9.32 shows the various mechanisms that influence the amount of radioactive material in each location inside the containment space at any point in time. A time-dependent inventory calculation is done for each important isotope. Figure 9.33 shows a typical result for iodine in air following a major release into containment for Bruce B. It can be seen that effective iodine trapping in the water is an important release-control mechanism. In the long term iodine in the form of organic iodides, which are difficult to filter, can be re-evolved into the air unless proper water chemistry conditions are maintained.
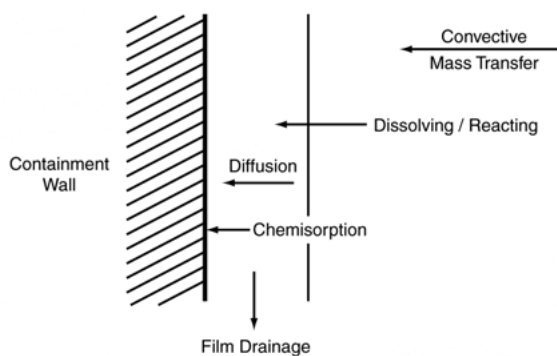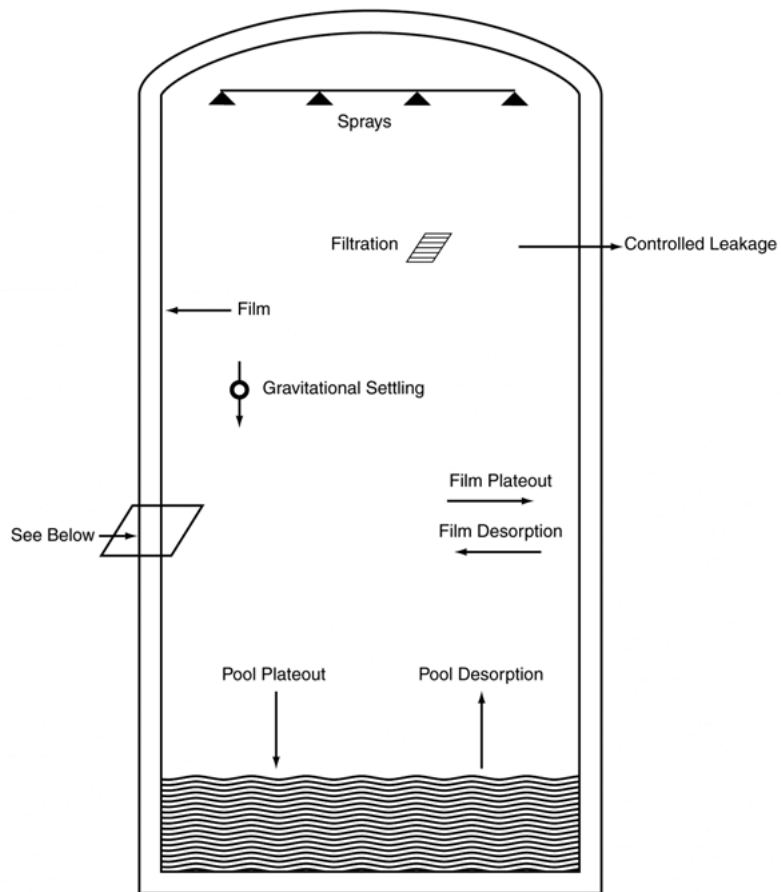
**FIGURE 9.32**
**NATURAL AND ENGINEERED MECHANISMS AFFECTING AIRBORNE**
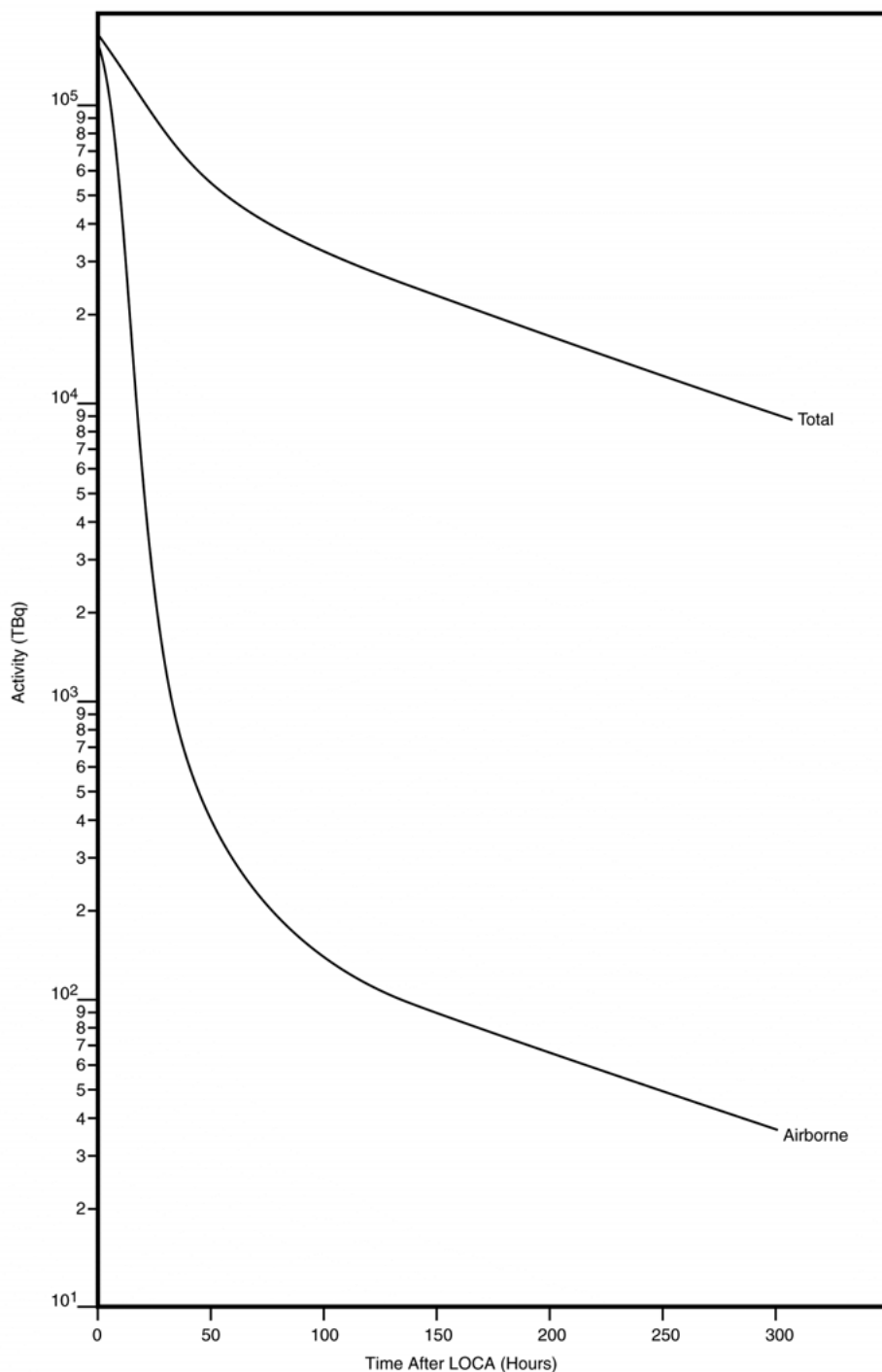**CONCENTRATION OF RADIONUCLIDES IN CONTAINMENT**

**FIGURE 9.33**
**IODINE ACTIVITY Vs. TIME FOLLOWING**
**LARGE BREAK LOCA**

PPI649 9-33

Figure 9.34 shows typical attenuation factors for iodine-131 for a major accident with intact containment envelope. Of the ten orders of magnitude reduction achieved, two orders can be attributed to emergency core cooling (ECI and moderator), three orders to the containment function, and five orders to atmospheric dilution from the release point to the site boundary.
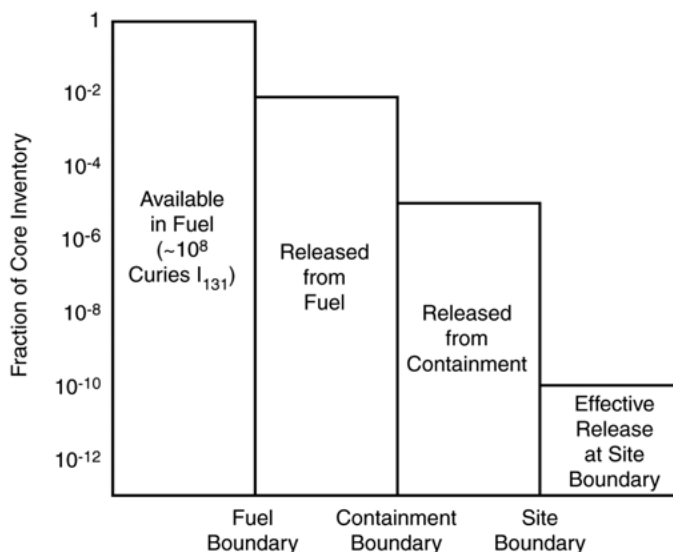


**FIGURE 9.34**
**TYPICAL ATTENUATION CANDU**
**(Large Break)**

Summary

This completes a brief outline of the factors to be considered, and methods which are used, to model the behavior of a CANDU plant following a loss of coolant accident. The prime purpose of these analyses is to test the capability of the safety system designs to limit the public consequences that might follow this kind of event. LOCA analysis is central to the safety design of any pressurized - coolant reactor, because of the fact that one of the barriers to fission product release is broken, the consequent reduction in fuel cooling, and the energetic release of coolant to the containment space. In the case of CANDU, this accident also leads to a reactivity increase in the core.

These analyses must not be taken to describe the expected sequence following an actual accident; they are only stylized models used to test the limits of protection systems capabilities. A real accident likely will arise from a special set of circumstances and will follow different pathways in space and time.